KfK 4376
Februar 1988

Texture Variations and Atomic Dislocations by Ar-Irradiation in Au and NbN Sputtered Layers

V. Jung
Institut für Nukleare Festkörperphysik

Kernforschungszentrum Karlsruhe

KERNFORSCHUNGSZENTRUM KARLSRUHE

Institut für Nukleare Festkörperphysik

KfK 4376

Texture Variations and Atomic Dislocations by Ar-Irradiation in Au and NbN Sputtered Layers

V. Jung

Büroexemplar
Kernforschungszentrum Karlsruhe GmbH
Nr.
1

Kernforschungszentrum Karlsruhe GmbH, Karlsruhe

Als Manuskript vervielfältigt
Für diesen Bericht behalten wir uns alle Rechte vor

Kernforschungszentrum Karlsruhe GmbH
Postfach 3640, 7500 Karlsruhe 1

ISSN 0303-4003

Abstract

Irradiation of Au and NbN sputtered layers with Ar^{++} ions of 600 keV leads to a narrower orientation distribution of the [111] direction of the Au layers from 12° FWHM to 6° and to only very small FWHM changes in texture distributions of the NbN layers. But the FWHM of the reflex distribution of the irradiated NbN layers is increased significantly from $\Delta\Theta = 0.65°$ to 1.17° for one sample position. This is caused by small atomic dislocations in the NbN lattice. The FWHM of reflex distribution of the Au layers increased only from $\Delta\Theta = 0.60°$ to 0.65° after irradiation. Oblique incidence of Ar^{++} ions causes, by absence of channeling, stronger distortions than perpendicular incidence.

Texturänderungen und atomare Verlagerungen durch Ar-Bestrahlung in Au und NbN Sputterschichten

Kurzfassung

Die Bestrahlung von aufgesputterten Gold- und NbN-Schichten mit Ar^{++}-Ionen von 600 keV führt zu einer schmaleren Orientierungsverteilung der Gold-Schichten von 12° FWHM zu 6° und zu sehr kleinen Änderungen der Halbwertsbreiten der Texturverteilungen der NbN-Schichten. Hingegen wird die Halbwertsbreite der Reflexverteilung der bestrahlten NbN-Schichten erheblich von $\Delta\Theta$ = 0.65° auf 1.17° für eine Probenposition vergrößert. Dies wird durch kleine statische Verlagerungen der Atome im NbN Gitter verursacht. Die Halbwertsbreite der Reflexverteilung der Goldschichten steigt durch Bestrahlung nur von $\Delta\Theta$ = 0.60° auf 0.65° an. Schiefer Einschuß der Ar^{++}-Ionen verursacht - dur Wegfall des Channeling - stärkere Störungen als senkrechter Einschuß.

1. Introduction

Superconducting materials will be used in large magnet coils for future fusion reactors, where they will be exposed to high radiation doses. Therefore, it is necessary to investigate the behavior of superconducting materials during irradiation.

The most important parameters of a superconductor are the superconducting transition temperature T_c, the critical magnetic field H_c, and the critical current density I_c, all being influenced by irradiation. The T_c of NbN sputtered layers, e.g. decreases from 16 K to 7 K after irradiation with 5×10^{17} Ar^{++}/cm^2. In new superconductors such as YBaCuO the critical current density is influenced by the texture of this material. If this material has grown in [001] direction normal to the substrate surface with a small FWHM of the texture distribution, the critical current density is maximum. If the material is polycrystalline and isotropic, the critical current density decreases substantially. For the critical field H_c a directional dependence will also exist.

Considering the directional dependence of superconducting properties it is useful to investigate variations of the texture of superconducting materials resulting from ion irradiation.

The NbN superconductor can be produced by sputtering NbN in nitrogen and argon atmosphere. Ar ions of 2 keV are focussed on an Nb target, and the sputtered Nb atoms together with the nitrogen in the argon atmosphere form NbN needles on e.g. a monocrystalline Al_2O_3 substrate. At a sputtering temperature of 800°C, an N_2 pressure of 4×10^{-3} Torr, and an Ar pressure of 2×10^{-2} Torr a stoichiometric NbN layer is formed. If the Al_2O_3 substrate is monocrystalline and is oriented e.g. with a $(11\bar{2}0)$ plane parallel to the surface plane, the [111] direction of the NbN layer will be mainly oriented normal to the surface plane of the substrate.

The lattice parameters of the hexagonal α-Al_2O_3 are $a = 4.758$ Å and $c = 12.991$ Å. The lattice parameters of the cubic Au and NbN are a = 4.09 Å and 4.39 Å, respectively. To get the distances of atoms in the (111) planes these parameters of the cubic lattices have to be divided and multiplied by $\sqrt{2}$, respectively, yielding to 2.89 Å and 6.22 Å. Compared with the above lattice parameters of α-Al_2O_3 the distance of atoms in [112] direction in the Au (111) plane parallel to parameter a in the Al_2O_3 $(11\bar{2}0)$ plane is to large by 5%. But the distance of atoms parallel to parameter c of the Al_2O_3 $(11\bar{2}0)$ plane is nearly exact: 2 c is nearly 9 distances of atoms in [110] direction in the Au (111) plane. This is shown in Fig. 1. However, for the NbN (111) plane there a mismatch results of 13%. In both cases (Au and NbN) the first (111) layers grow epitaxially by deformation of the atomic distances. But, the following layers no more can be correlated exactly and a fiber texture will result for the following Au and NbN atomic layers. The FWHM of this two-dimensional fiber texture is 6° ... 16° depending on the sputtering temperature. The higher the sputtering temperature is the smaller is the FWHM which results for a one-dimensional section through the [111] NbN pole sphere. In most cases the sputtering temperature was between 700° and 850° C.

2. Irradiation of NbN and Au layers

In a fusion reactor a high flux of fast neutrons collides with the atoms of the superconducting material causing displacements and dislocations of atoms. Given the small mass of the neutron, the energy transfer to the atoms of e.g. an NbN lattice is relatively low. The fraction of the primary energy of the colliding particle which is transferred to the atom in a central collision is:

$$f = \frac{4\, M_1 \times M_2}{(M_1 + M_2)^2}$$

with M_1 = mass of colliding particle and M_2 = mass of atom in the lattice

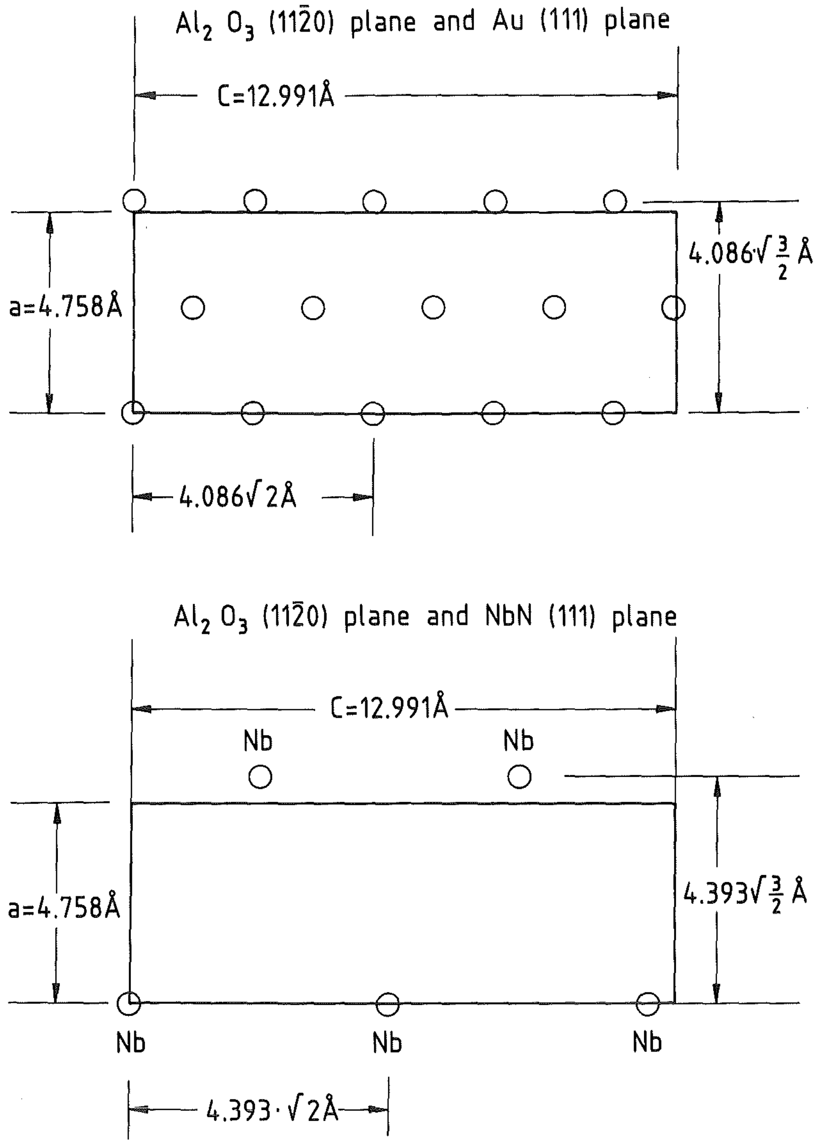

Fig. 1 Mismatch between the Al_2O_3 (11$\bar{2}$0) plane and the Au (111) plane and the NbN (111) plane.

In order to shorten the exposure time a large energy transfer is necessary. Therefore, the irradiation is suitably performed with atoms of medium weight, e.g. Ar atoms. The energy transfer from Ar atoms to N atoms in a central collision is 35% of the primary energy, from an Ar atom to an Nb atom 89%, and from an Ar atom to an Au atom 55%.

If Au is irradiated, the damage in the Au lattice is much smaller than in NbN. This is due to two important reasons: 1. The energy transfer from Ar to Au is smaller. 2. The melting point of Au is much lower than that of refractory materials such as NbN. On account of the second reason damages in gold lattices are annealed faster than in NbN lattices. Due to this irradiation induced differences in the behavior of NbN and Au lattices it was suitable to perform irradiation experiments on NbN layers and on Au layers for comparison.

During irradiation the ion bombardment produces resputtering of the layers. In case of NbN after a dosis of 1.25×10^{17} cm² ca. 30% of a 2000 Å thick NbN layer is removed. In case of an 800 Å thick Au layer the layer was totally dissolved after the last irradiation step. To avoid the channeling effect this irradiation was carried out at an angle of incidence of 75°. All samples (Au and NbN) were irradiated at 75° (oblique incidence) and at 90° (normal incidence). In case of 90° incidence the incoming Ar atoms, due to channeling, suffer very small energy loss and therefore the damage of the lattices is much smaller. The half angle of the angular region where channeling takes place is 1.5° for NbN and increases to about 5° for Au because of the $\sqrt{Z}$ dependence and other dependencies, e.g. lattice parameter.

3. Texture measurements with a two-axes diffractometer

The knowledge of the whole Orientation Distribution (ODF) of a crystalline material requires the intensities to be measured of several reflexes on the whole pole sphere (Bunge, 1982).

A fiber texture is rotationally symmetric with respect to a preferred sample axis. Hence, it is sufficient to measure only one-dimensional cuts of the pole spheres of the material to be investigated. This was also done in previous measurements made on an 18/8 CrNi round steel to study the effect of texture inheritance by neutron diffraction (Jung, 1983). In the present investigation two sections of one pole figure were used (without ODF calculation). In usual texture measurements the sample is tilted around an axis, which lies in the diffractometer plane and this axis is normal to the diffractometer axis. In the measurement reported here, the sample is rotated around the diffractometer axis. If the rectangular sample is positioned parallel or transverse to the diffractometer axis two sections through the pole sphere are obtained which are orthogonal to each other.

The Au and NbN sputtered layers investigated were grown on monocrystalline sapphire substrates oriented with a $(11\bar{2}0)$ plane parallel to the surface plane of the substrate. The [111] direction of the grown Au and NbN layers is distributed around the normal direction of the substrate. If the orientation of the Al_2O_3 $(11\bar{2}0)$ plane is not exactly parallel to the surface plane, e.g., oblique by an angle of 1°, the orientation distribution of the sputtered layers (Au or NbN) deviates by this same small angle because of the epitaxy between substrate and layer.

If the misalignment of the substrate is less than 1° in one or two dimensions - transverse and parallel to the rectangular size of the substrate - and if the FWHM of the texture distribution is about 11° or more, it is sufficient to measure changes of sections through the pole sphere in two dimensions only, which are transverse to each other. The error in the FWHM of a section through the pole sphere is 3%, if the misalignment is 1° and the FWHM of the section is 11°. This is shown in Fig. 2.

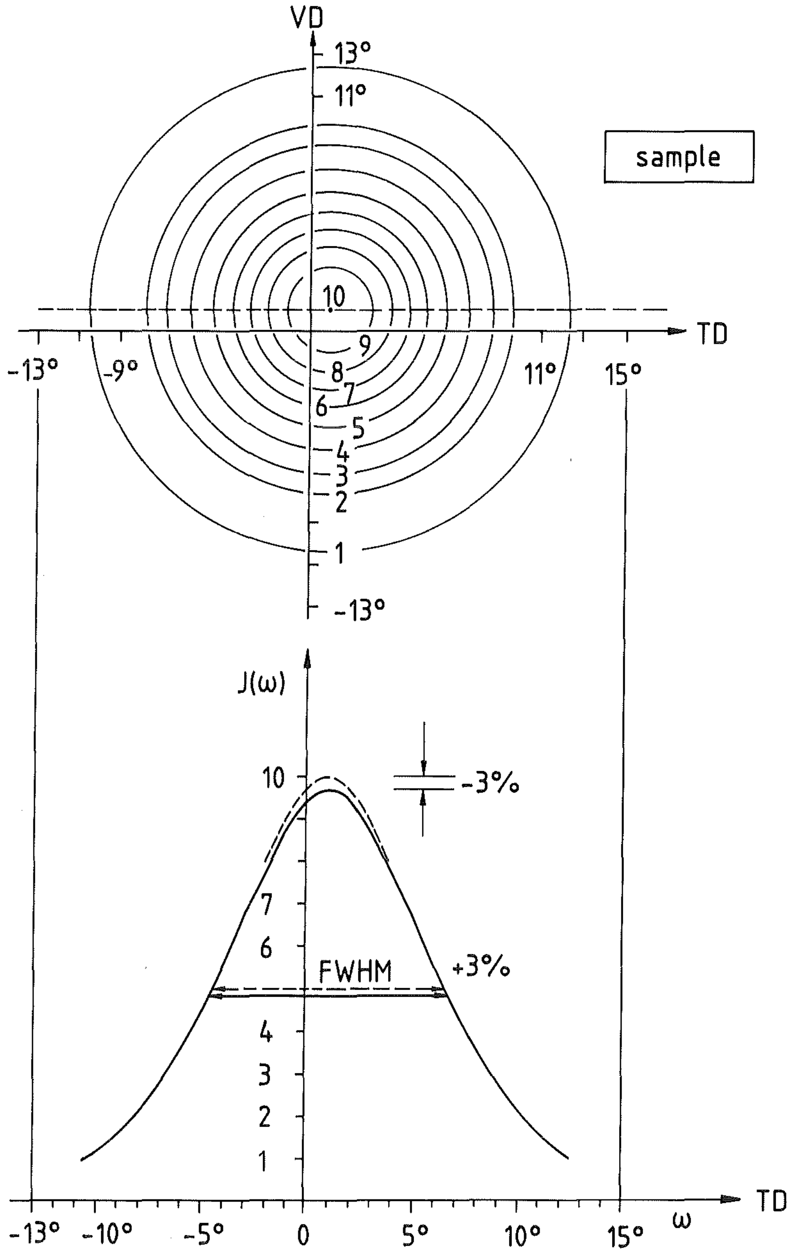

Fig. 2 Pole figure of a fiber texture with misalignment of the maximum of the distribution by 1° in both directions (transverse direction = TD, vertical direction = VD) of the rectangular sample.
A cut through the pole sphere in this case produces a FWHM, which is increased by 3%. With the used two-axes diffractometer and its sample holder it only was possible to get sections through the pole sphere normal on VD and normal on TD. A section along the dashed line would produce the true FWHM of the texture. Beyond the pole figure the section through the pole sphere is shown.

With a two-axis diffractometer texture measurements also are possible, if the misalignment of the orientation distribution due to the misalignment of the substrate in one dimension is 3° ... 5°, but is zero in the dimension orthogonal to the first. When texture measurements at such a misaligned layer, e.g. NbN, are performed, only one section through the [111] pole figure meets the maximum of the texture distribution. The maximum of the second cut through the pole sphere then is importantly decreased compared with the first section (see Fig. 2).

Because of the two positions of the sample in the diffractometer (transverse or vertical) and because of the extension of the X-ray in vertical direction on the sample (10 mm parallel to the diffractometer axis) different areas of the sample are selected for measurement. By this it is possible that a region is met with nearly homogeneous lattice parameter distribution. And orthogonal to the first position of the sample a region can be met with a large lattice parameter variation. In the unirradiated state both positions of the sample (transverse and vertical) show the same reflex FWHM. But after irradiation by 2.5×10^{16} Ar^{++}/cm^2 a different broadening of the reflex distribution FWHM from $\Delta\Theta = 0.65°$ to $\Delta\Theta = 1.17°$ has been found for the vertical position of the rectangular sample and from $\Delta\Theta = 0.65°$ to $\Delta\Theta = 0.85°$ for the transverse sample position. This difference is caused by irradiation induced strain in the lattice.

4. Measurements

Gold layers of 800 Å thickness on oriented sapphire substrates were irradiated at intervals with 600 keV Ar^{++} ions. Thereby the layer thickness is reduced due to desputtering. The intervals of irradiation dose were chosen in such a manner that it was possible to recognize small irradiation induced variations of texture of the layers which provided useful information. To achieve this, irradiation steps whose doses differed from each other by a factor 5 were chosen.

The first dose applied was 2 x 10^{14} Ar^{++}/cm^2. As the gold layers were only 800 Å thick the layer was completely dissolved by the undesired desputtering during irradiation when the last dose of 10^{17} Ar^{++}/cm^2 was applied by injection at an angle of 75° so that channeling effects did not appear. However, in case of vertical (90°) injection because of channeling effects a measurable rest was left.

Due to the greater thickness of the measured NbN layers (2000 Å) only about 35% of the layer thickness was removed after the last bombardment. The thickness of the layers was chosen to a dimension that the Ar ions did not stop in the layer and the layers were damaged homogeneously.

In earlier experiments made on NbN layers a minor difference had already been found between vertical (90°) injection and oblique injection (75°) respectively (Jung, 1986, 1987). In this case one sample was broken into two parts. The two parts of the same sample were irradiated at 90° and at 75°, respectively. Accordingly, oblique injection causes the orientation distribution of the NbN [111] direction to undergo greater changes than vertical injection which is especially noticeable when the last dose is applied, i.e. 2.5 x 10^{16} to 1.25 x 10^{17} Ar^{++}/cm^2. This result is shown in Fig. 3.

Whereas in case of vertical injection the FWHM of the orientation distribution increases from 7.2° to 7.3°, i.e., by only 0.1°, the width of distribution of the same section through the pole sphere in case of oblique injection increases from 6.8° to 7.3°, i.e., by 0.5° in the other part of the same sample.

This higher efficiency of oblique injection is attributed to the disappearance of channeling. Ions hitting parallel to the [111] direction make much lesser collisions than ions deviating by 5° from this [111] direction. In case of gold layers the channeling angular range is increased by $\sqrt{Z_{Au}/Z_{Nb}}$ and by different lattice parameter and by the fact that in the NbN

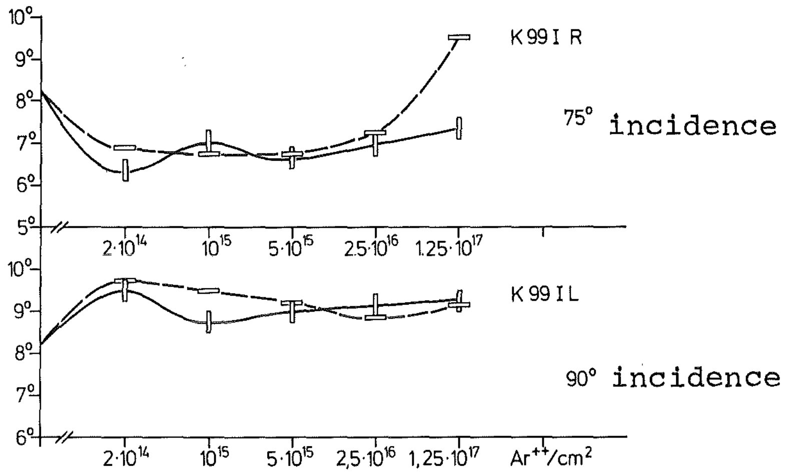

Fig. 3 The FWHM of the texture distribution of NbN layers in dependence on the Ar irradiation dose. The transverse rectangle gives the transverse position of the sample and the vertical rectangle gives the vertical position of the sample. Two parts of the same, not homogeneous sample were irradiated by oblique (75°) and perpendicular (90°) injection. This causes different variation of FWHM in dependence on the irradiation dose.

lattice each second atom has a Z of only 7. This fact implies that on vertical injection a still measurable residue of the gold layer remained on the substrate after application of an integrated irradiation dose of 1.25×10^{17} Ar^{++}/cm^2 whereas in case of injection at 75° the gold layer was dissolved by the Ar irradiation without any residue left.

The layer thickness of the irradiated layers had been measured by backscattering of protons, which were analyzed in a multichannel analyzer. When the range of these protons is twice the layer thickness, half of the number of backscattered protons were absorbed in the layer. The range straggling of the protons produces no sharp corner in energy spectrum of the backscattered protons, but in this way a very exact determination of the remaining layer thickness is possible (Chu, Mayer and Nicolet, 1978).

Only under certain conditions the integrated reflectivity can be taken as the measure of the remaining layer thickness. Integrated reflectivity is understood here to mean the triple integral of intensity over the one-dimensional reflex distribution and over the two-dimensional orientation distribution of the assumed fiber texture. In the investigated cases there was no isotropic fraction and the FWHM of the cuts through the pole spheres was very narrow (6° ... 12°). That means that it is sufficient to have a small area of the whole pole sphere as integration region. This method turns out false when an isotropic fraction of the investigated material is existent. If the distribution of the reflex becomes broader, the intensity in the maximum of the reflex decreases inversely proportional to the widening of the intensity distribution of the reflex with the total intensity of the reflex remaining constant.

If, however, the two-dimensional distribution of orientation of the assumed fiber texture becomes equally broader to the same extent in the two directions orthogonal to each other (two sections through the pole sphere), the intensity in the maximum of the orientation distribution decreases inversely proportional to the square of the broadening factor of the orientation distribution. The integrated reflectivity was calculated from data measured - width of reflex and the two widths of section through the pole sphere (two one-dimensional orientation distributions) of the [111] direction (see Fig. 2) - and the value obtained was normalized to unity for the unirradiated material.

The measurements were performed with a two-axes crystal diffractometer by X-ray diffraction with CuK_α-radiation. If the maximum of distribution of the [111] direction occurs close (1° ... 2°) to the surface normal of the substrate, it will in most cases suffice to lay two sections through the [111] pole sphere orthogonal to each other (see Fig. 2).

Since a texture goniometer was not available, a Philips two-axes diffractometer was used for texture measurement for one cut through the pole sphere of the [111] direction. The primary beam-defining divergence was 1/6°, which produces an irradiated area on the sample of 0.3 mm transverse to the diffractometer axis and of 10 mm parallel to the diffractometer axis. In Fig. 4 the angles Θ and ω are defined. If $\Theta - \omega$ = 10°, the width of the irradiated area will increase up to 1.5 mm. This does not cause a loss of intensity and the Bragg-condition is not disturbed, because the detector - with a defining divergence of 4° - covers the whole irradiated sample area.

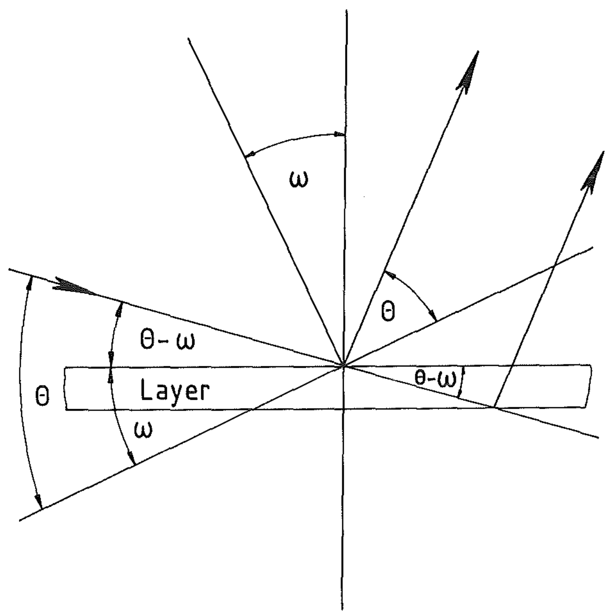

Fig. 4 Definition of the angles ω and Θ. The effective path length through the layer is: layer thickness divided by $\sin(\Theta-\omega)$. Therefore the measured X-ray intensity values have to be corrected by multiplication with $\sin(\Theta-\omega)$. The layer thickness is very small against the penetration depth of the X-rays.

Because of the small layer thickness which is small compared with the penetration depth of the X-rays it is sufficient to multiply the values of the measured intensity by $\sin(\Theta-\omega)$, because the effective path through the layer is layer thickness divided by $\sin(\Theta-\omega)$. The corrections which have to be applied to the measurements for larger layer thickness have been described in earlier reports (Jung, 1986; International Tables, 1967).

5. Results and discussion

Fig. 5 shows the results of the measurement made on gold layers. In the top part the reflex intensity in the maximum of the texture distribution (orientation distribution) is shown for the two sections through the pole sphere. The two values marked by a vertical and a transverse rectangle differ a little bit. This might be caused by different reasons, e.g., the texture distribution is not equally reduced in the two cuts through the pole sphere. Because the variation of the reflex distribution of the gold layers by irradiation is small, the value of the reflex maximum is a measure for the whole reflex intensity. And the plotted values are the maxima of the reflex distributions.

The reflex intensity in the maximum of reflex distribution and in the maximum of texture distribution between the unirradiated state and a dose of 1.25×10^{17} Ar^{++}/cm^2 has two maxima and a more constant tendency for perpendicular incidence, while it increases for oblique incidence in dependence on the irradiation dose (at top Fig. 5).

In the center the integrated reflectivity in dependence on the irradiation dose is shown. The integrated reflectivity is normalized to unity for the not irradiated state.

The integrated reflectivity is a measure for the distortion of the crystallites of the layer and should not be used for determination of remaining layer thickness.

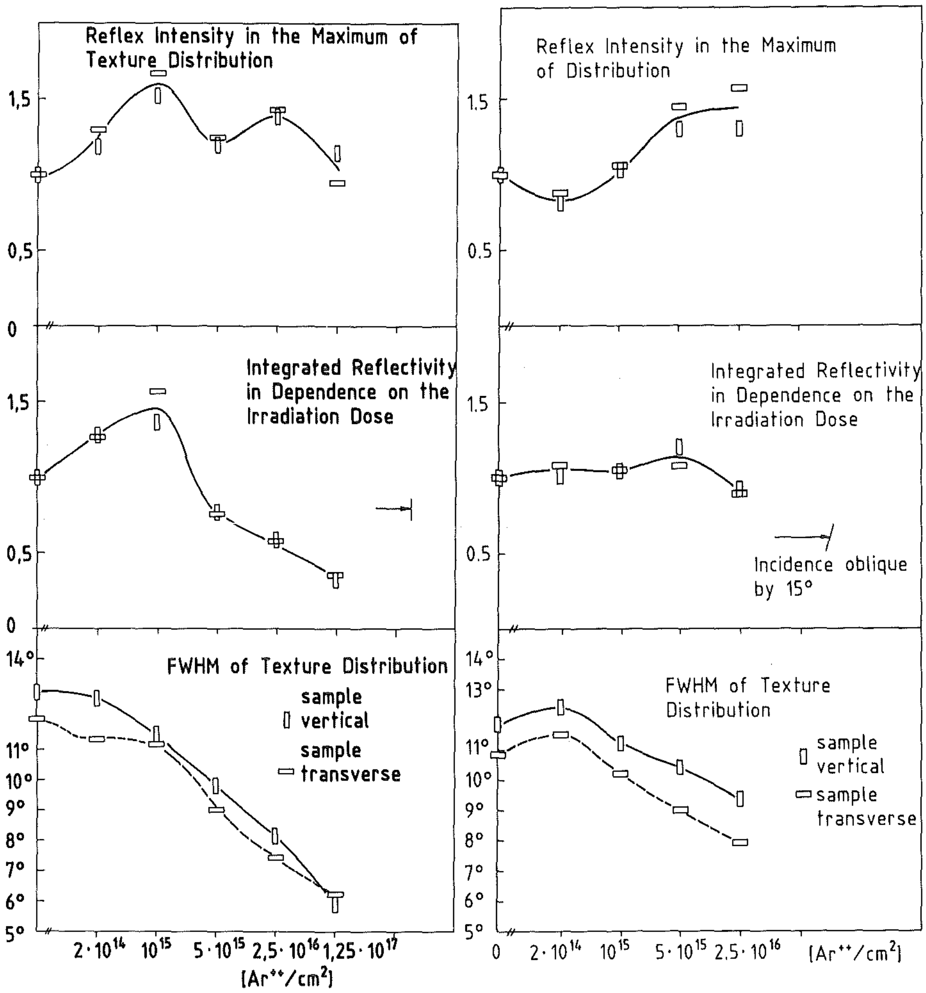

Fig. 5 Results of the measurements on gold layers of 800 Å with perpendicular and oblique incidence of Ar^{++}-ions. The texture distribution of the [111] direction of one not irradiated layer has a FWHM of 12° and 13° for vertical and transverse sample position, respectively. After irradiation by 1.25 x 10^{17} Ar^{++}/cm^2 the FWHM decreases to 6° in case of perpendicular incidence (left bottom).

In order to find out whether a single cut through the pole sphere is sufficient to determine the integral reflectivity, the values of integral reflectivity were determined separately for the two cuts orthogonal to each other. The value measured in the maximum of texture distribution must then be multiplied by the broadening factor of the reflex distribution and, in addition, by the square of the reduction or broadening factors, respectively, of texture distribution cuts.

For the gold layers measured, the reduction factors diminishing the FWHM of texture distribution are different for the transversal and vertical directions of cuts only at a dose of 10^{15} Ar^{++}/cm^2. Therefore, according to the calculations, different values of the actually identical integral reflectivity are obtained at this dose level, as regards the vertical and transversal sample positions, respectively.

The integrated reflectivity has a very different result for perpendicular and oblique incidence (in the middle of Fig. 5). The plot of the integral reflectivity as a function of the irradiation dose can be explained as follows: the unirradiated gold layer consists of relatively perfect crystals. Therefore the X-radiation is partly extincted. To the extent to which the crystallites suffer from damage, the integral reflectivity increases until it reaches a maximum at a dose of 10^{15} Ar^{++}/cm^2. Then reduction of layer thickness by sputtering dominates when irradiation continues. In case of oblique injection (right side, center) the maximum is attained only at a dose of 5×10^{15} Ar^{++}/cm^2. Then the integral reflectivity begins to decrease due to reduction in the layer thickness.

The bottom part of Fig. 5 is a plot of the widths of orientation distributions in two cuts through the [111] pole sphere orthogonal to each other. The left hand side (90° injection) and the right hand side (75° injection) show significant differences. These are caused mainly by the channeling effects at 90° injection. Both cases (90° and 75° injection) have in common the strong reduction in the width of the [111] orientation distribution in the two cuts orthogonal to each other.

In order to illustrate the decrease of texture width, Fig. 6 shows the two cuts through the [111] pole sphere orthogonal to each other, both for the unirradiated gold layer (at top) and the irradiated gold layer (at bottom). As it is improbable that by irradiation islands are formed on the substrate with narrower distribution of orientation, it could be concluded that the FWHM of the orientation distribution of the gold layer incrases with increasing layer thickness. And when the upper layers are sputtered away by Ar irradiation the FWHM of the remaining layer therefore becomes smaller. But a measurement of the FWHM of texture distributions of gold layers with different layer thickness - sputtered at same conditions - show an opposite tendency. The FWHM of texture distribution of a gold layer of 400 Å thickness was 17°, while the FWHM of the distribution of a layer with 800 Å thickness was only 10°. Both layers were sputtered at same conditions (700°C). It is sure that recrystallization takes place during Ar irradiation in the gold layer. The most probable reason for the decrease of texture distribution cut FWHM from 12° to 6° is the fact, that the lattice parameter of the Ar irradiated Au layer is decreased by 2%. This means that the mismatch between the lattice parameter a of Al_2O_3 and a $\sqrt{3/2}$ of the Au layer is reduced from 5% to 3%.

The behavior of an NbN layer is completely different in case that similar irradiation doses are applied. Recrystallization, if any, takes place to a very low extent only. However, contrary to the gold layer, the crystal structure is heavily disturbed by static dislocation of atoms after Ar irradiation. This can be recognized from an extremely strong widening of the reflex distribution FWHM from $\Delta\Theta = 0.65°$ in the unirradiated state to $\Delta\Theta = 1.17°$ for the vertical position of the sample after irradiation with 2.5×10^{16} Ar^{++}/cm^2. The increase in the transverse sample position (another sample region) was from $\Delta\Theta = 0.65°$ to $\Delta\Theta = 0.85°$.

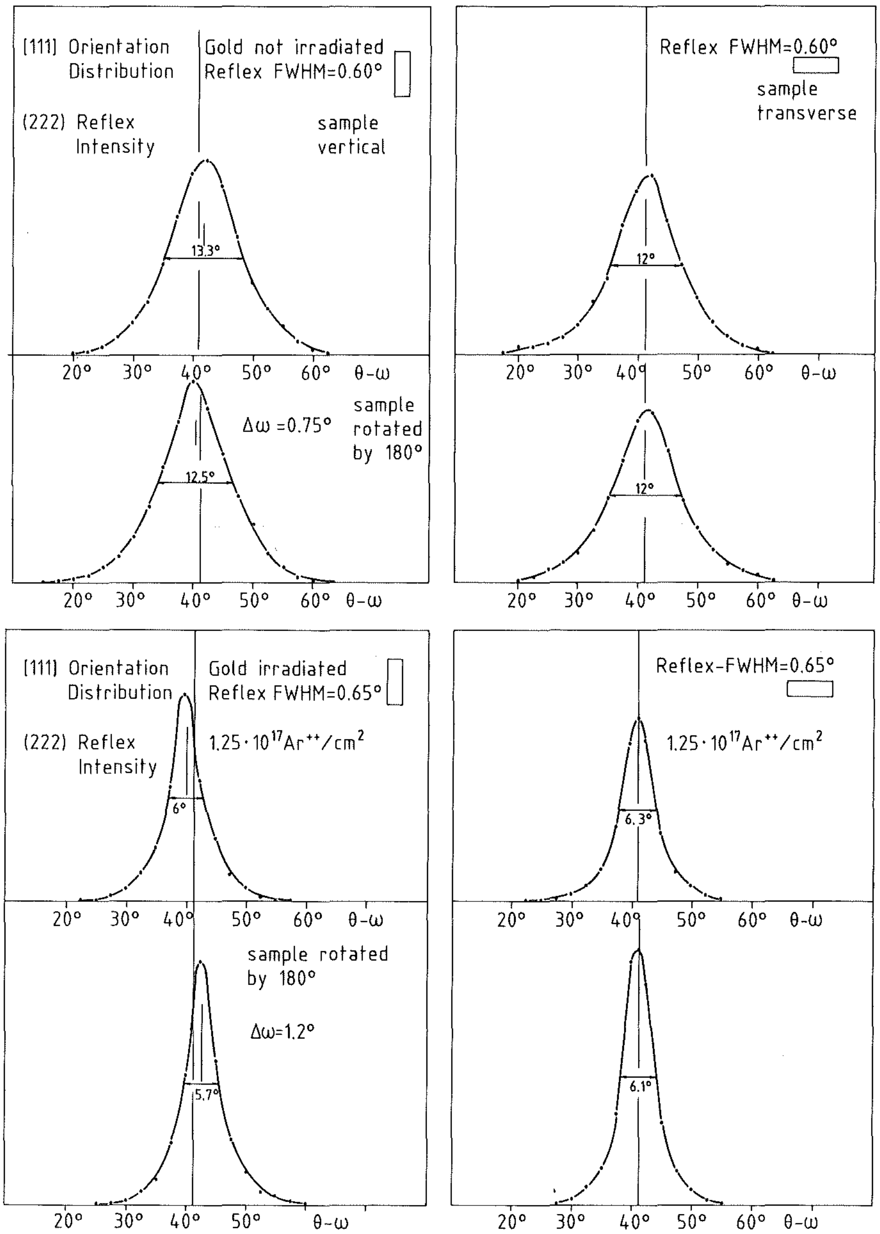

Fig. 6 Two orthogonal cuts through the pole sphere of the gold [111] direction for not irradiated (top) and for irradiated (bottom) gold layer. Each cut has been measured a second time after rotation of the sample by 180° around an axis normal to the layer, and from both maxima of the cuts the mean value has been taken for the plot in Fig. 5. At $\Theta = 41°$ ω was 0. The maximum of the [111] direction distribution in one cut is oblique by 0.75° and 1.2° with and without irradiation, respectively.

This means that refractory materials as NbN are very resistant to changes in texture after irradiation whereas in gold layers the crystal structure is resistant to irradiation. The lower melting point of gold leads to annealing of damages.

Fig. 7 shows, for comparison with the measurements made on gold layers (Fig. 5), the result of measurements performed on a NbN layer with 90° incidence. Whereas the integrated reflectivity of the gold layers above a dose of 5×10^{15} Ar^{++}/cm^2 decreases as the layers become thinner due to resputtering by irradiation, the integrated reflectivity of the NbN layer slightly tends to increase for the vertical sample position.

At the measured NbN layer the vertical and the transverse cuts through the [111] pole sphere exhibit very different broadening or reduction factors, respectively, of texture distribution cuts (Fig. 7 at bottom). The differences are much more conspicuous in the FWHM of reflex distribution in the maxima of texture distribution cuts, as sayed above. But also the intensities of the reflex in the maximum of reflex distribution and in the maxima of texture distribution cuts are different for the two cuts orthogonal to each other (Fig. 7, top). This asymmetry becomes understandable if one takes into account that the area of the sample in the two-axis diffractometer met by the X-ray is different for vertical and transverse sample position, respectively. The X-ray has a vertical extension of 10 mm and of 0.3 ... 1.0 mm transverse to the diffractometer axis. All measurements are carried out at the same areas, each for vertical and transverse sample position, respectively. Thus, only a small area is the same for both positions (vertical and transverse), because wobbling of the sample was not possible at this used diffractometer. Reduction of the vertical extension of the X-ray from 10 mm to 1 mm would lead to an increase of the measuring time by a factor 10.

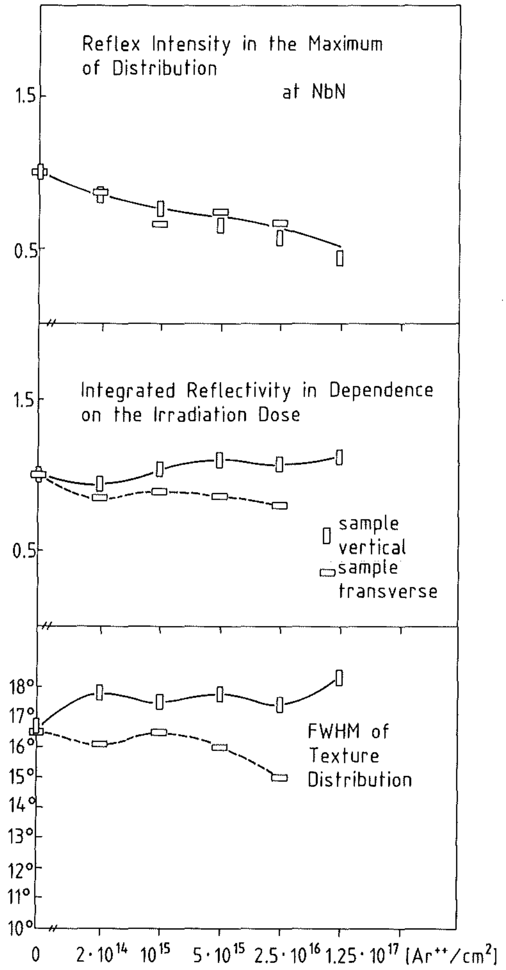

Fig. 7 Results of irradiation of an NbN layer by Ar^{++}-ions at 90° incidence. The FWHM of the [111] direction distribution has only a very small dependence on the irradiation dose (bottom). The integrated reflectivity also has small variation (middle). But the increase of the reflex FWHM from $\Delta\Theta = 0.65°$ to $\Delta\Theta = 1.17°$ for the vertical sample position leads to a decrease of the reflex intensity in the maximum of the reflex distribution taken in the maximum of the [111] orientation distribution cut (at top). All values are different for vertical and transverse sample positions, respectively, because different areas are met by the X-ray on the sample for vertical and transverse sample position, respectively.
The maximum of the orientation distribution is met only for the vertical sample position. That means that the vertical rectangles represent more valid values of measurement than the horizontal rectangles.

Compared with the Au layers the irradiated NbN layers are very inhomogeneous. This inhomogeneity is pronounced by the different increase of the reflex distribution FWHM from $\Delta\Theta = 0.65°$ to $\Delta\Theta = 1.17°$ for the vertical sample position and from $\Delta\Theta = 0.65°$ to $\Delta\Theta = 0.85°$ for the transverse sample position. As pointed out in chapter 3, the lattice parameter distribution is not the same in both sample directions orthogonal to each other. It might be possible that the misalignment of a $(11\bar{2}0)$ plane of the sapphire substrate by 3.5° in the vertical sample direction (see Fig. 2) has an influence on this inhomogeneity. This fact shows that the integrated reflectivity of the damaged layers can not be taken as a measure for the layer thickness. The result enables the conclusion to be drawn that the NbN crystal structure is heavily disturbed because a reduction in layer thickness must be considered in addition. Thus the measurements on gold layers confirm the conclusions drawn from measurements on NbN layers.

Διαιρέσεις δὲ χαρισμάτων εισίν, τὸ δὲ αυτὸ πνεῦμα· καὶ
διαιρέσεις διακονιῶν εισίν, ὁ δὲ αυτὸς κύριος· καὶ
διαιρέσεις ἐνεργημάτων εισίν, ὁ δὲ αυτὸς θεὸς ὁ ἐνεργῶν
τὰ πάντα ἐν πᾶσιν.

(1. Kor. 12, 4-6)

In memoriam Prof. Günter Wassermann

Acknowledgement

The author is very grateful to Prof. Dr. Dr. h.c. H.-J. Bunge for his critical reading of this work and to Dr. O. Meyer for the propose to perform measurements at Au layers.

Furthermore the author would like to thank R. Smithey for the sputtering of NbN and Au layers and B. Strehlau for the irradiation of these layers with Ar ions.

References

Bunge, H.-J. and Esling, C.: Quantitative Texture Analysis. Editor: Deutsche Gesellschaft für Metallkunde e.V., Oberursel 1982.

Chu, W.K., Mayer, J.W., and Nicolet, M.-A.: Backscattering Spectrometry, Academic Press, New York 1978.

International Tables for X-Ray Crystallography, Vol. II, pp. 301-306. The International Union of Crystallography, Birmingham 1967.

Jung, V.: Arch. Eisenhüttenwes. 54, Nr. 11, pp. 453-460 (1983).

Jung, V.: Variations of NbN Surface Textures by Ar^{++}-Irradiation Taking into Account Variations of Reflex Distribution. Theoretical Methods of Texture Analysis, Clausthal, March 17-22, 1986. Editor: H.-J. Bunge, Deutsche Gesellschaft für Metallkunde e.V., Oberursel, pp. 183-188 (1987).

Jung, V.: Zeitschrift für Kristallographie, 174, pp. 107-109 (1986).

Jung, V.: Texture Measurements with a Two-Axis-Diffractometer. Experimental Techniques of Texture Analysis, March 25-29, 1985. Editor: H.-J. Bunge, Deutsche Gesellschaft für Metallkunde e.V., Oberursel, pp. 265-274 (1986).